



Modelling of Coupled Temperature Field in Multi-Modal Thermal Process and Its Analytical Solutions

Xiaoli Liu¹, Ling Jin^{1*}, Jing Gao¹, Sunyufei Wang²

¹ Jitang College, North China University of Science and Technology, Tangshan 063210, China

² College of Chemical Engineering, North China University of Science and Technology, Tangshan 063210, China

Corresponding Author Email: jinling@ncst.edu.cn

<https://doi.org/10.18280/ijht.410118>

ABSTRACT

Received: 5 November 2022

Accepted: 20 January 2023

Keywords:

multi-modal thermal process, coupled temperature field, analytical solution, thermal power plant, cross entropy

To keep the main system and the auxiliary equipment of production system of thermal power plants operating normally, it's a necessary work to fully consider the periodical repeat features of thermal process when modelling the thermal process based on thermal state data of machine units. Since most equipment in power plant work in an electromagnetic coupling environment, a too high ambient temperature will affect the safe operation of units, so when studying the dynamic features of multi-modal thermal process of power plants and their soft environment, the temperature distribution features of multi-modal thermal process should be classified. To solve these questions, this paper established a model for the coupled temperature field during multi-modal thermal process and studied its analytical solutions. At first, this paper proposed a multi-modal modelling method for solving the distribution features of coupled temperature during multi-modal thermal process, the method can quickly determine the optimal number of local models of multi-modal thermal process of power plant units while reducing the computational load of the coupled temperature field model. Then, this paper introduced an improved niche method into the basic cross-entropy optimization algorithm and used it to solve the layout optimization problem of coupled temperature field during multi-modal thermal process. At last, the validity of the proposed method was verified by experimental results.

1. INTRODUCTION

In a power system, the thermal power plants serving as power suppliers are one of the most important links [1-4]. Their function is to complete the energy form transformation of fuel from chemical energy, to the thermal potential energy of steam, then to mechanical energy, and finally to electric energy. Boiler, steam turbine, and generator are called the three main equipment in thermal power plants [5-11], other auxiliary equipment of production system includes the coal delivery system, the chemical treatment system of water, and the slurry discharge system, etc. These systems cooperate with the main system to complete the task of electricity production [12-15]. To ensure these equipment to operate normally, it's a necessary work to fully consider the periodical repeat features of thermal process of power plants [16-19] when modelling the thermal process based on thermal state data of machine units, thereby promoting the units to develop toward the direction of multi-parameter, multi-modal, and highly automated.

Zhang et al. [20] introduced a novel monitoring method of multi-modal dynamic processes based on sparse dynamic inner principal component analysis. In their work, by adopting the concept of intelligent synapses in continual learning, a loss of quadratic term was introduced to penalize the changes of mode-related parameters, and modified synaptic intelligence was proposed to estimate the importance of these parameters. Then, authors also discussed the features of the proposed method, including computational complexity, advantages and

potential limitations. At last, compared with several advanced monitoring methods, the effectiveness and superiority of the proposed method were demonstrated by a continuous stirred tank heater case and a practical industrial system. Grigor'ev et al. [21] optimized the structure and parameters of an autonomous hybrid power plant operating from renewable energy sources (sun and wind) and methanol fuel cells using mathematical models of thermal processes, then they applied the developed models in practice and gave the results of simulation experiments of an indicated power plant. Weng et al. [22] pointed out that typical thermal processes are usually monotonically responsive and can be well described by first-order plus dead time (FOPDT) model, thus the system identification of FOPDT is a major concern in the field of thermal process control, including coal-fired power plants and gas turbines. However, step response based open-loop experiment is sometimes not available due to the limitation of field operation, which necessitates the development of closed-loop identification. Authors employed artificial intelligence to derive a new method for closed-loop identification, and used Convolution Neural Network (CNN) to identify operation characteristics of devices in the closed-loop condition. Their experimental results proved that the application of CNN had dramatically improved identification accuracy; when the size of training datasets reached 50,000, the identification accuracy was higher than 98%.

Most equipment in power plants work in an electromagnetic coupling environment, a too high ambient temperature will affect the safe operation of units, so when studying the

dynamic features of multi-modal thermal process of power plants and their soft environment, the temperature distribution features of multi-modal thermal process should be classified. To solve these questions, this paper established a model for the coupled temperature field during multi-modal thermal process and studied its analytical solutions.

2. MODELING OF MULTI-MODAL THERMAL PROCESS

There are a few shortcomings with existing modeling method of coupled temperature field for multi-modal thermal process: 1) Termination conditions are unreasonably designed; 2) Feature information contained in sample set are not fully utilized, and it's easy to pick noise data by mistake; 3) The validity evaluation index of multi-modal data clustering is not effectively utilized, which may result in redundancy of the multi-modal model.

To overcome these shortcomings, this paper proposed an optimized multi-model modeling method for analyzing distribution features of coupled temperature during multi-mode thermal process, the method can quickly determine the optimal number of local models of multi-modal thermal process of power plant units while reducing the computational load of the coupled temperature field model.

Conventional methods usually pick two samples with the lowest similarity in the data set of multi-modal thermal state as the initial cluster centers, different from these existing methods, the multi-modal modelling method proposed in this paper based on fuzzy satisfaction clustering could fully consider the time-varying characteristics of multi-modal thermal process. Starting from the internal feature information of the data of sample set, the proposed method determines the initial cluster center via Singular Value Decomposition (SVD) to attain ideal clustering results. That is, at first, this method calculates the unit eigenvector and standard deviation of the covariance matrix of multi-modal thermal state data; then, based on the calculation results, it selects two sample points around the center point of sample set and takes them as the initial cluster centers. The proposed method can control the core features of the sample set of multi-modal thermal state data in the data expansion direction, and quickly complete the classification of sample set by taking the iteration advantage of clustering analysis.

The original multi-modal thermal state data matrix C composed of original unit thermal state data samples can be written as:

$$C = \begin{bmatrix} \phi_1(1) & \cdots & \phi_K(1) & b(1) \\ \phi_1(2) & \cdots & \phi_K(2) & b(2) \\ \vdots & \ddots & \vdots & \vdots \\ \phi_1(M) & \cdots & \phi_K(M) & b(M) \end{bmatrix} \quad (1)$$

By performing centralization and scale transformation operations on C , we have:

$$C^* = \begin{bmatrix} \tilde{\phi}_1(1) & \cdots & \tilde{\phi}_K(1) & \tilde{b}(1) \\ \tilde{\phi}_1(2) & \cdots & \tilde{\phi}_K(2) & \tilde{b}(2) \\ \vdots & \ddots & \vdots & \vdots \\ \tilde{\phi}_1(M) & \cdots & \tilde{\phi}_K(M) & \tilde{b}(M) \end{bmatrix} \quad (2)$$

where,

$$\tilde{\phi}_j(l) = \frac{\phi_j(l) - n_{\phi_j}}{\phi_{j,MAX}}, \quad j = 1, 2, \dots, K; l = 1, 2, \dots, M;$$

$$\tilde{b}(l) = \frac{b(l) - n_b}{b_{MAX}}, \quad l = 1, 2, \dots, M$$

$$n_{\phi_j} = \frac{1}{M} \sum_{i=1}^M \phi_j(i), \quad j = 1, 2, \dots, K;$$

$$n_b = \frac{1}{M} \sum_{i=1}^M b(i)$$

$$\phi_{j,MAX} = \max_l \left(|\phi_j(l) - n_{\phi_j}| \right), \quad j = 1, 2, \dots, K;$$

$$b_{MAX} = \max_l \left(|b(l) - n_b| \right)$$

$u_0 = T_{1 \times (K+1)}$ is the center of the sample set of multi-modal thermal state data C^* , $u_0 = [n_{\phi_1}, \dots, n_{\phi_K}, n_b]$ is the center corresponding to the original multi-modal thermal state data matrix C , then the covariance matrix G_0 corresponding to C^* can be calculated:

$$G_0 = \frac{1}{M-1} C^{*T} C^* \quad (3)$$

Assuming: E_{0j} represents the unit eigenvector of G_0 , $\mu_{0j}(j=1, 2, \dots, K+1)$ represents the corresponding eigenvalues, through SVD, E_{0j} and $\mu_{0j}(j=1, 2, \dots, K+1)$ can be calculated:

$$G_0 = \begin{bmatrix} e_{01}, \dots, e_{0(K+1)} \end{bmatrix} \text{diag} \left(\mu_{01}, \dots, \mu_{0(K+1)} \right) \begin{bmatrix} e_{01}, \dots, e_{0(K+1)} \end{bmatrix}^{-1} \quad (4)$$

The eigenvalue μ_{0j} of G_0 describes the variance of C^* in direction E_{0j} . Assuming: $\mu_{0,max}$ represents the maximum eigenvalue of the sample set of multi-modal thermal state data, $E_{0,max}$ represents the principle eigenvector, the main direction of data expansion of sample set is the direction of $E_{0,max}$, in this direction, the variance $\varepsilon_{0,max}^2$ around u_0^* is equal to $\mu_{0,max}$.

Let ξ_1 be equal to $\varepsilon_{0,max} e_{0,max}$, which can be used to describe the data expansion information of the sample set, then the two initial cluster centers u_{11}^0 and u_{12}^0 of C^* are:

$$u_{11}^0 = -\xi_1, u_{12}^0 = \xi_1 \quad (5)$$

Based on C^* , u_{11}^0 , and u_{12}^0 , the G - K algorithm can be used to cluster the unit state data. If the coupled temperature field model identified based on clustering results does not meet precision requirements, then the number of clustering categories d needs to be increased. Figure 1 shows the generation of new cluster center. Assuming: C_q^* represents the worst multi-modal thermal state data sample sub-set determined by current iteration; G_q represents its covariance matrix, u_q represents the cluster center, $e_{i-1,max}$ represents the maximum unit eigenvector calculated by SVD, $\varepsilon_{i-1,max}$ represents the corresponding standard deviation of the data, then delete u_q , and let $\xi_i = \varepsilon_{i-1,max} e_{i-1,max}$, and define a new cluster center as follows:

$$u_{i1}^0 = u_q - \xi_i, u_{i2}^0 = u_q + \xi_i \quad (6)$$

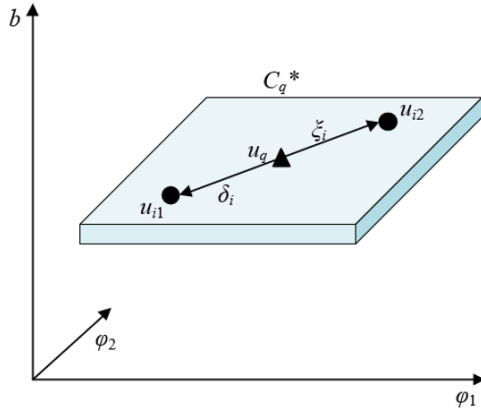


Figure 1. Generation of new cluster center

After clustering was finished, by transforming u_q into the coordinates of original unit thermal state data, the structure parameters (N, d_i, ε_i) of the coupled temperature field model could be determined further, wherein N is the number of local models of multi-modal thermal state, namely d :

$$N=d \quad (7)$$

d_i ($i=1, 2, \dots, N$) is the center of the scheduling function, namely the fuzzy cluster center formed by transforming the first K items of u_i into the coordinates of original unit thermal state data, which is denoted as $u_{i\psi}$.

$$u_i = [u_{i1}, \dots, u_{iK}, u_{ib}] \Rightarrow d_i = u_{i\psi} = [\phi_{1,MAX} u_{i1} + n_{\phi_1}, \phi_{K,L,MAX} u_{iK} + n_{\phi_K}], i = 1, 2, \dots, d \quad (8)$$

Assuming: $u_{k\psi}$ ($1=1, 2, \dots, L$) represents L centers closest to the i -th center $u_{i\psi}$, α_d is a constant used to adjust the width of

the Gaussian function, then ε_i ($i=1, 2, \dots, N$) is determined by the mean distance between u_i and the nearest L centers.

$$\varepsilon_i = \frac{1}{\alpha_d} \left(\frac{1}{L} \sum_{l=1}^L \|u_{i\psi} - u_{k\psi}\| \right), i = 1, 2, \dots, d \quad (9)$$

Define $I_p=[1,1,\dots,1]^T$, $I_p \in R^p$, the formula below gives the applicable domain of the i -th local model:

$$\Lambda_i \in [d_i - \varepsilon_i I_p, d_i + \varepsilon_i I_p], i = 1, 2, \dots, N \quad (10)$$

Figure 2 shows the flow of the proposed modeling method.

3. ANALYTICAL SOLUTIONS OF THE LAYOUT OPTIMIZATION PROBLEM OF COUPLED TEMPERATURE FIELD

This paper chose to use the cross-entropy optimization algorithm to solve the layout optimization problem of coupled temperature field during multi-modal thermal process. Taking the model constructed in the previous section as the subject, this paper introduced an improved niche method into the basic cross-entropy optimization algorithm for the purpose of improving the validity of the analytical solutions of the coupled temperature field model of multi-modal thermal process. Figure 3 shows the flow of algorithm for solving the analytical solutions. Expressions of the species formation strategy and crowding strategy of the niche method are given below. Assuming: R_i represents the i -th niche, E represents the rest population, a_j represents individuals in E , a_{best} represents the optimal individual in E , s represents niche radius, C represents the dimension of design space, $DIS(x, y)$ represents the distance between individuals x and y , then there are:

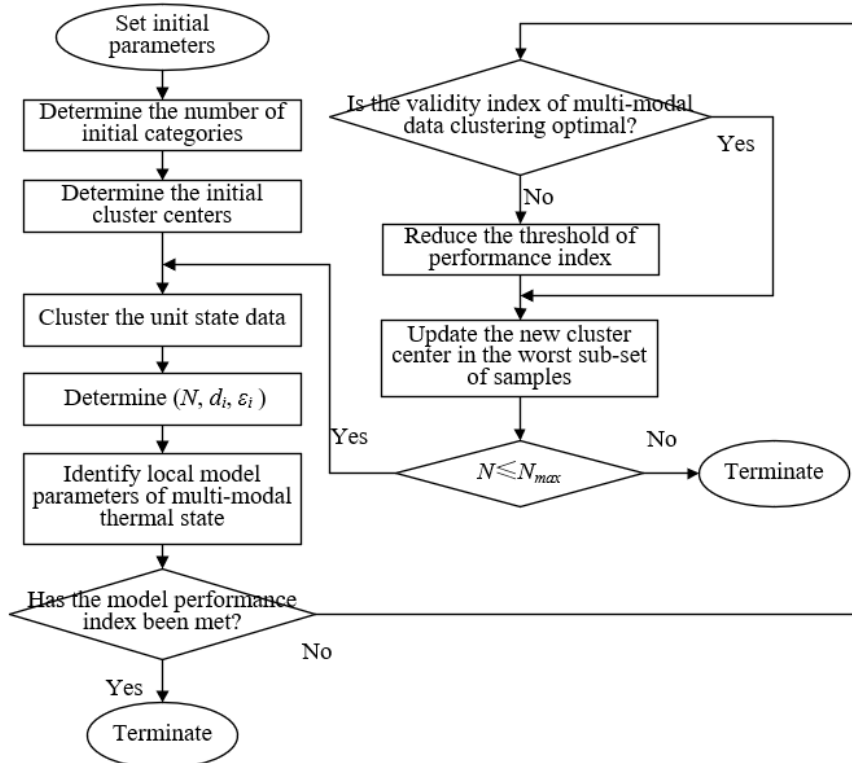


Figure 2. Flow of the proposed modeling method

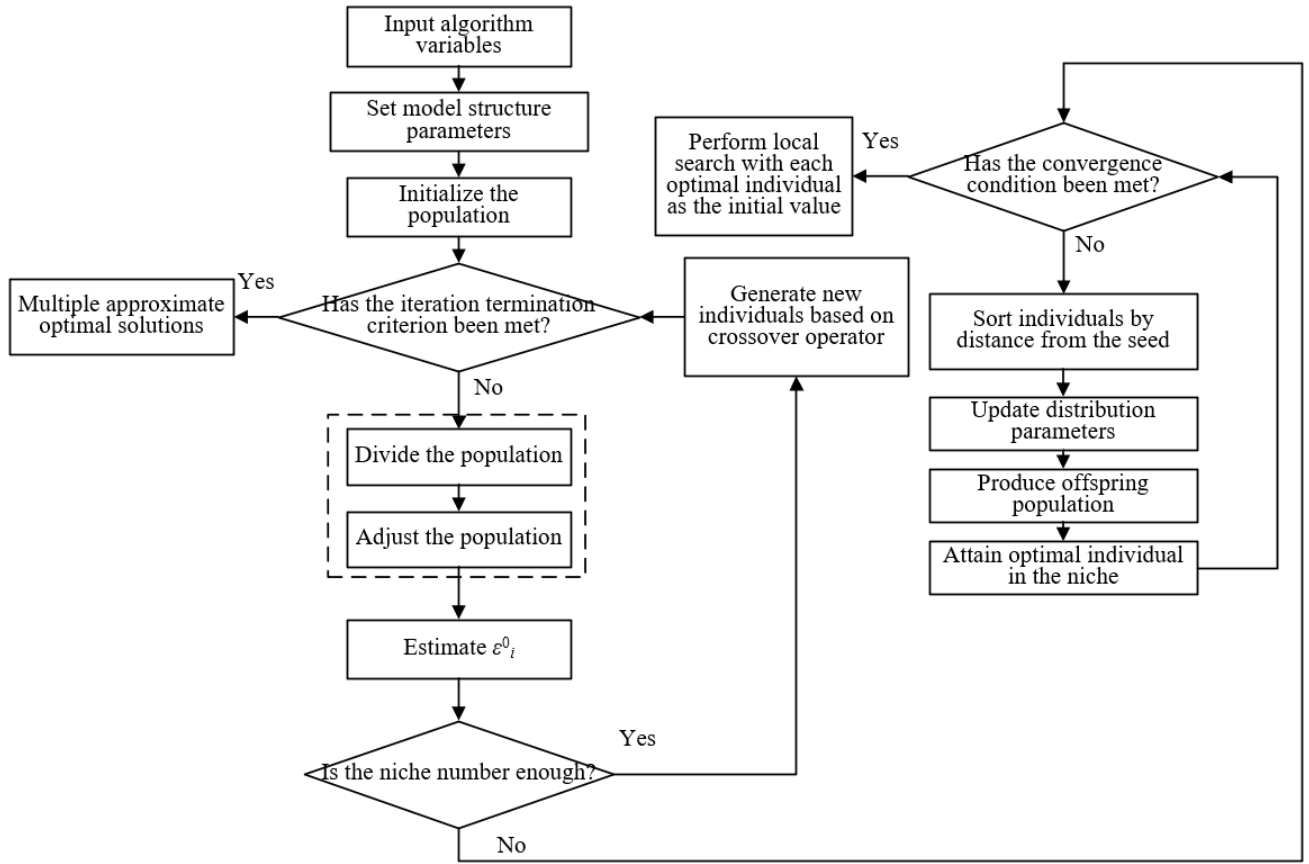


Figure 3. Flow of algorithm for solving analytical solutions

$$R_i = \left\{ DIS(a_{best}, a_j) = \sqrt{\sum_{c=1}^C (a_{best}^c - a_j^c)^2} \leq s \right\} \quad (11)$$

$$\arg \min_{a_j \in D_i} DIS(a_j, a_{best}) = \sqrt{\sum_{c=1}^C (a_{best}^c - a_j^c)^2} \quad (12)$$

Overall speaking, the attained analytical solutions of coupled temperature field model for multi-modal thermal process face many challenges. The first is the determination of niche radius and the challenge of algorithm parameters, in the meantime, it also needs to bear a huge computational load and maintain population diversity. Therefore, at first, this paper performed adaptive clustering on niche radius, and adopted elite strategy and local search to complete the estimation of distribution parameters, at last, the crossover operator was adopted to generate new niche individuals. After optimization, the algorithm's ability to solve analytical solutions of the temperature field model had been greatly enhanced.

The adaptive clustering process of niche radius can be divided into two steps: dynamic population division of niche radius, and population adjustment based on same scale. At first, the optimal individual was taken as the seed and other individuals were sorted according to their distance from the seed, then the adaptability values of neighbor individuals were compared. If a worse individual is encountered, then the adaptability value of the niche radius can be determined based on the distance between this individual and the seed. The following formula gives the judgment criterion:

$$f(x_i) > f(x_{i-1}) \quad (13)$$

To balance the exploration and development of the population, the population divided into multiple clusters was adjusted based on the same scale, that is, if a cluster contains more individuals, then poor individuals contained in it are eliminated; if a cluster contains less individuals, then new niche individuals are produced.

The estimation of distribution parameters of the algorithm includes two parts: the estimation of position selection λ_i of the optimal individual, and the estimation of initial standard deviation ε^0_i and standard deviation $\varepsilon^0_i(t>0)$. To improve the convergence speed of the algorithm, assuming: a_{ibest} represents the optimal individual in the i -th niche, if λ_i is selected to be a_{ibest} , then there is:

$$\lambda_i = a_{i,best} \quad (14)$$

Assuming: β represents the variance coefficient associated with upper and lower limits, in order to attain effective solution of the algorithm in the first round of iteration, this paper introduced β to control the distribution of initial population, finally, effective sampling of the individuals had been completed.

$$\varepsilon_{i,c}^0 = \frac{1}{\beta} \times (vy(c) - ky(c)) (c = 1, 2, \dots, C) \quad (15)$$

To provide sufficient multi-modal thermal state data sample information, the calculation of standard deviation $\varepsilon^0_i(t>0)$ needs to be performed based on all individuals in the niche. Assuming: k_i represents all individuals in the niche, m_i represents the size of population in the i -th niche, then there is:

$$\varepsilon_i^2 = \frac{\sum_{m \in k_i} (a - \lambda_i)^2}{m_i} \quad (16)$$

The performance of multi-model modeling strategy has a great impact on the global peak number of analytical solutions of the temperature field model searched by the cross-entropy optimization algorithm. At the same time, the diversity of population declined sharply during algorithm iteration. To avoid the loss of population diversity, this paper used the crossover operator between the optimal individuals in each niche to produce new niche individuals. Specifically, keeping the total population size ME unchanged was taken as the objective, by referring to the size of niche a_{best} , the rest $ME - m_{best}$ new individuals were produced. Assuming: a_j^c and a_i^c represent the optimal individual in the i -th and j -th niche, a_i^c represents new individuals generated by the crossover operator, C represents the dimension of design variable, then there is:

$$a_i^c = a_j^c + rand(\) \times (a_i^c - a_j^c) \quad (c = 1, 2, 3, \dots, C) \quad (17)$$

4. EXPERIMENTAL RESULTS AND ANALYSIS

Some data samples of multi-modal thermal state were listed, it's set that the maximum number of allowable local models of multi-modal thermal state was 5. Figure 4 shows the initial cluster centers of multi-modal thermal state data sample set determined by the proposed method and the cluster center attained based on G-K clustering. The comparison given in this paper showed that the proposed method is effective and reasonable, it can control the main features of the sample dataset of multi-modal thermal state in the data expansion direction, and ensure that the algorithm can find the optimal clustering center of the sample set quickly and accurately.

Figure 5 shows the variation of validity index under the condition of different category numbers. When the initial threshold of the performance index was given a small value, although the validity index of clustering reached local minimum value at a category number of 3, the modelling accuracy at this time was not satisfactory enough. When the initial threshold of the performance index was adjusted to a

larger value, the modelling accuracy met requirements at a category number of 5, the validity index of clustering was ideal, and the modelling process terminated. To ensure successful modeling, the threshold of performance index should be adjusted smaller referring to the validity index of clustering, otherwise ideal model accuracy won't be realized even if the number of local model reaches the preset maximum value. Table 1 gives the specific system model parameters.

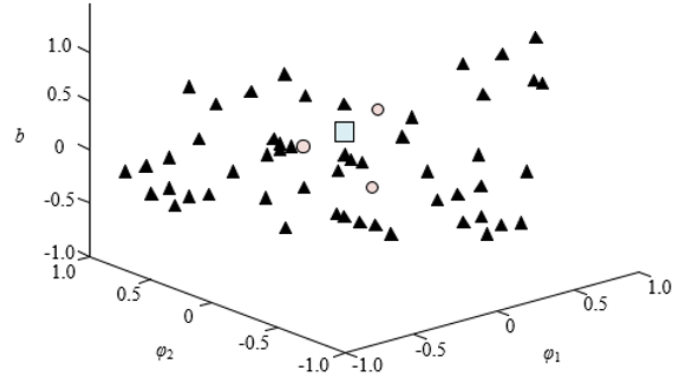


Figure 4. Clustering of non-linear data samples of multi-modal thermal state

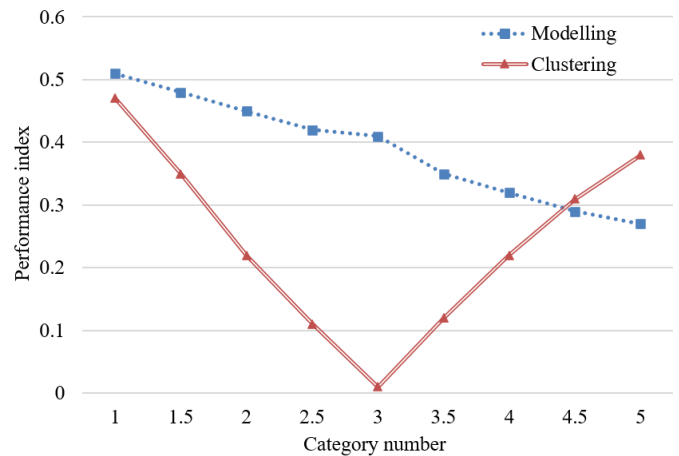


Figure 5. Validity index under different category numbers

Table 1. System model parameters

| Model number | Parameters of scheduling function | | | Parameters of local models | | |
|--------------|-----------------------------------|----------|-----------------|----------------------------|-------------|-------------|
| | d_{i1} | d_{i2} | ε_i | χ_{i0} | χ_{i1} | χ_{i2} |
| 1 | 3.9521 | 4.1753 | 1.3453 | 5.0854 | -0.4736 | -0.3319 |
| 2 | 1.5987 | 3.6758 | 1.2736 | 8.8123 | -1.9357 | -0.7618 |
| 3 | 3.5329 | 1.7284 | 1.2459 | 7.2617 | -0.5723 | -1.4317 |
| 4 | 1.6874 | 1.5923 | 1.1736 | 10.4358 | -2.1736 | -1.9524 |

Table 2. Comparison of system modeling accuracy

| Model | Number of local models | Model error |
|-------------------------|------------------------|-------------|
| Piece-wise affine model | 7 | 0.081 |
| T-S fuzzy model | 11 | 0.0145 |
| Local model network | 5/6 | 0.113/0.103 |
| The proposed method | 5/6 | 0.062/0.035 |

Table 2 compares the accuracy of the proposed model and other models in terms of the target multi-modal thermal process system, as can be known from the table, the proposed

model exhibited obvious advantages in terms of accuracy and local model number.

For the purpose of fair comparison, a same initial population size and a same calculation times of maximum objective function were set for all algorithms used in this study to solve the analytical solutions of the layout optimization problem of coupled temperature field. The proportion of elite samples in the multi-modal thermal state sample dataset was set to 0.1, and the settings of other parameters are given in Table 3.

To evaluate the advantage of the proposed method in solving the analytical solutions of the layout optimization problem of coupled temperature field, this paper compared it

with other algorithms. The selected reference algorithms include several classic optimization algorithms, such as ant colony optimization (ACO) algorithm, particle swarm optimization (PSO) algorithm, bacteria foraging optimization (BFO) algorithm, firefly algorithm (FA), artificial fish swarm algorithm (AFSA), and artificial bee colony (ABC) algorithm.

Moreover, this paper also compared the proposed algorithm 1 (before adaptive clustering of niche radius) with the proposed algorithm 2 (before introducing elite strategy and local search to perform distribution parameter estimation) to verify the improvement effect of the conventional niche algorithm.

Table 3. Model parameter settings

| Sample No. | Calculation times of maximum objective function | Population size | Number of correct predictions | Coefficient of variance |
|------------|---|-----------------|-------------------------------|-------------------------|
| 1 | 5.1E+4 | 90 | 30 | 1/35 |
| 2 | 2.1E+4 | 110 | 30 | 1/35 |
| 3 | 2.1E+4 | 310 | 30 | 1/35 |
| 4 | 4.1E+4 | 310 | 30 | 1/35 |
| 5 | 2.1E+4 | 10 | 30 | 1/35 |
| 6 | 2.1E+4 | 210 | 30 | 1/35 |
| 7 | 4.1E+4 | 210 | 60 | 1/35 |
| 8 | 4.1E+4 | 210 | 110 | 1/35 |
| 9 | 4.1E+4 | 210 | 110 | 1/35 |

Table 4. Optimal analytical solutions of different algorithms

| Algorithm | Unit 1 | | Unit 2 | | |
|--------------------------|-------------------|-------------------|-------------------|-------------------|-------------------|
| | Measuring point 1 | Measuring point 2 | Measuring point 1 | Measuring point 2 | Measuring point 3 |
| ACO | -2.0915 | -2.7358 | -0.0209 | -0.0112 | 0.257 |
| PSO | 0.0035 | 0.5137 | 0.0000 | -0.1436 | -0.0241 |
| BFO | -0.1723 | 1.4465 | 0.0223 | -0.0145 | 0.0135 |
| FA | -1.5734 | -1.4578 | 0.0157 | -0.0085 | 0.0023 |
| AFSA | -0.4712 | 0.0239 | -0.2675 | -0.2736 | -0.1935 |
| ABC | 0.2357 | 0.5671 | -0.0453 | -0.0106 | -3.50E-06 |
| The proposed algorithm 1 | -1.2735 | 2.4941 | -0.0213 | 0.0229 | -0.0127 |
| | -2.3675 | 1.1445 | 0.0025 | -0.0045 | 4.472E-02 |
| The proposed algorithm 2 | -0.0134 | 0.1024 | 2.53E-05 | -3.89E-06 | 0.1153 |
| | -1.2257 | 0.8938 | 0.0046 | 0.0125 | 0.00589 |
| | 0.2512 | 0.3857 | 0.0083 | -0.0113 | 0.0176 |
| The proposed algorithm | 0.3359 | 2.0592 | -0.0142 | -4.937E-05 | 0.0145 |
| | -2.5359 | 1.3605 | 0.0165 | -0.0053 | 0.0123 |
| | -2.7512 | 0.1574 | -0.0089 | 0.0114 | -0.0037 |
| | 0.3157 | -1.1731 | -0.0251 | 0.0067 | 0.0019 |

Table 4 gives the statistical results and the optimal results of the proposed algorithm and reference algorithms in solving the analytical solutions of the layout optimization problem of coupled temperature field, as can be seen from the data in the table, the proposed algorithm performed better than other reference algorithms.

The population size of the improved niche algorithm used in the paper was respectively adjusted to 100, 200, and 400 to solve the temperature field layout optimization problem of all equipment in the target unit, and four optimal threshold values of 2.6, 2.7, 2.8, and 2.9 were set. Figure 6 shows the number of optimal analytical solutions attained by the proposed algorithm. As can be seen from the figure, when the population size of the niche algorithm was set as 200 or 400, the proposed algorithm gave more competitive advantages of multi-modal optimization performance of unit thermal process state in terms of solving analytical solutions of the layout optimization problem of couple temperature field. When the optimal threshold was 2.7, the proposed algorithm could get more than 130 different optimal analytical solutions in a single iteration, which had verified that the proposed algorithm attained more excellent multi-modal optimization ability in case of larger population size.

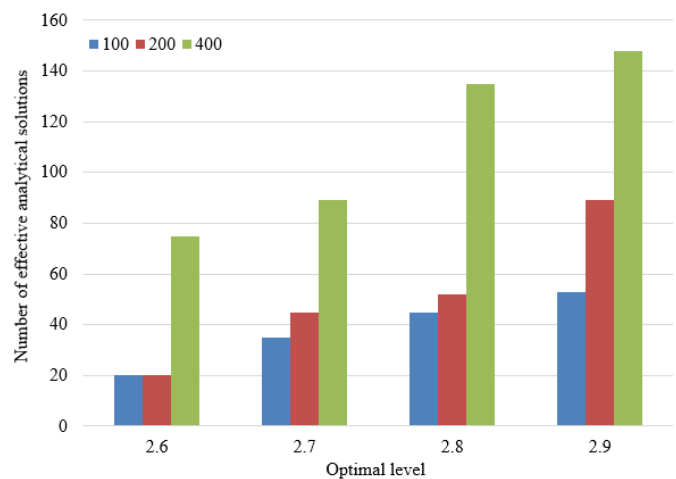


Figure 6. Number of optimal analytical solutions attained by the proposed algorithm

5. CONCLUSION

This paper modeled the coupled temperature field in multi-modal thermal process and studied its analytical solutions. At first, an improved modelling method was proposed for

analyzing the distribution features of coupled temperature in multi-modal thermal process, the method can quickly determine the optimal number of local models of multi-modal thermal process of power plant units while reducing the computational load of the coupled temperature field model. Then, an improved niche method was introduced into the basic cross-entropy optimization algorithm for the purpose of solving the layout optimization problem of coupled temperature field in multi-modal thermal process.

In the experiment, the clustering of nonlinear data samples of multi-modal thermal process state was given, and the results proved the proposed modeling method is reasonable and effective. Then, the variation of validity index under the condition of different category numbers was given; for the target multi-modal thermal process system, the modeling accuracy of the proposed model and other models was compared, and the results verified the obvious superiority of the proposed model in terms of accuracy and number of local models. Moreover, the optimal results of the proposed algorithm and a few reference algorithms in solving the layout optimization problem of coupled temperature field were shown, and the results demonstrated that the proposed algorithm had outperformed other reference algorithms. At last, this paper analyzed the number of optimal analytical solutions attained by the proposed algorithm and the conclusion indicated that the proposed algorithm attained more excellent multi-modal optimization ability in case of larger population size.

ACKNOWLEDGEMENT

The construction and research of “New Medicine” curriculum system under the background of artificial intelligence (Project Number 202101040001).

REFERENCES

- [1] Deng, Y., Zhu, Z., Wang, W., Ye, Q., Yu, B., Sun, D. (2023). Numerical analysis and optimization of the charging process on a shell-and-tube latent heat thermal energy storage unit for a solar power plant with direct steam generation. *Energy Science & Engineering*, 11(1): 206-226. <https://doi.org/10.1002/ese3.1323>
- [2] Sultanov, M.M., Boldyrev, I.A., Evseev, K.V. (2022). Application of machine learning to predict the thermal power plant process condition. *Journal of Physics: Conference Series*, 2150: 012029. <https://doi.org/10.1088/1742-6596/2150/1/012029>
- [3] Xin, N., Wicaksono, A.P. (2022). Green development approach of chemical water treatment process in thermal power plant. In 2022 IEEE Sustainable Power and Energy Conference (iSPEC), Perth, Australia, pp. 1-5. <https://doi.org/10.1109/iSPEC54162.2022.10032997>
- [4] Filimonova, A., Chichirov, A., Chichirova, N., Batalova, A. (2022). Organic substances in process waters of a thermal power plant with a combined cycle gas turbine plant and methods for their detection. In *Proceedings of ICEPP 2021: Efficient Production and Processing*, Kazan, Russia, pp. 247-256. https://doi.org/10.1007/978-3-030-86047-9_26
- [5] Prabu, D., Giriprasath, A., Viknesh, S. (2020). Design and development of a prototype thermal power plant for recycling of sea water by distillation process. *IOP Conference Series: Earth and Environmental Science*, 573: 012014. <https://doi.org/10.1088/1755-1315/573/1/012014>
- [6] Vlasova, A.Y., Vlasov, S.M. (2020). Research on acid and high-mineralized wastewater neutralization and purification process of the thermal power plant (TPP) ionite water treatment plants on laboratory stand. *Journal of Physics: Conference Series*, 1652: 012006. <https://doi.org/10.1088/1742-6596/1652/1/012006>
- [7] Ardghail, P.M., Leen, S.B., Harrison, N.M. (2020). A review of thermal, microstructural and constitutive modelling of 9Cr steel for power plant applications: Towards a through-process model for structural integrity of welded connections. *International Journal of Pressure Vessels and Piping*, 180: 104037. <https://doi.org/10.1016/j.ijpvp.2019.104037>
- [8] Singh, S.P., Ghosh, S.K., Dwivedi, V.K. (2020). An Analytic hierarchy process (AHP)-based multi-criteria evaluation and priority analysis for best FWH substitution of solar aided thermal power plant. In *Proceedings of International Conference in Mechanical and Energy Technology: ICMET 2019, India*, pp. 707-717. https://doi.org/10.1007/978-981-15-2647-3_66
- [9] Madejski, P., Michalak, P., Karch, M., Kuś, T., Banasiak, K. (2022). Monitoring of Thermal and Flow Processes in the two-phase spray-ejector condenser for thermal power plant applications. *Energies*, 15(19): 7151. <https://doi.org/10.3390/en15197151>
- [10] Kvascev, G.S., Djurovic, Z.M. (2022). Water Level Control in the Thermal Power Plant Steam Separator Based on New PID Tuning Method for Integrating Processes. *Energies*, 15(17): 6310. <https://doi.org/10.3390/en15176310>
- [11] Zhao, H., Zhu, W., Ye, H., Dong, H. (2022). Research on synchronous optimization of steam power system for processing units and thermal power plant operation. *Chemical Industry and Engineering Progress*, 41: 44-53.
- [12] Wang, Y., Zhou, D., Chen, M. (2023). Dynamic related component analysis for quality-related process monitoring with applications to thermal power plants. *Control Engineering Practice*, 132: 105426. <https://doi.org/10.1016/j.conengprac.2022.105426>
- [13] Ruling, H., Lin, L., Qing, C., Yan, G., Tao, L. (2021). Transient simulation model and process simulation analysis of fast cut back process in thermal power plant. *Journal of Physics: Conference Series*, 1754: 012144. <https://doi.org/10.1088/1742-6596/1754/1/012144>
- [14] Wang, Q., Tang, M., An, A., Qiu, J., Zhang, K., Liu, W. (2021). Hierarchical control modeling of thermal power plant production process based on MAS. In 2021 China Automation Congress (CAC), Beijing, China, pp. 835-840. <https://doi.org/10.1109/CAC53003.2021.9727837>
- [15] Didenko, N.I., Skripnuk, D.F., Bobodzhanova, L.K., Hazov, V.K. (2021). Management of the design and construction process of a thermal power plant under conditions of permafrost instability. *IOP Conference Series: Earth and Environmental Science*, 625: 012022. <https://doi.org/10.1088/1755-1315/625/1/012022>
- [16] Yu, X., Liu, Y., Zhou, Y., Wang, Y., Zhang, Y., Zhu, Y. (2020). Simulation study on urea thermal decomposition for SCR process of thermal power plant. *IOP Conference Series: Earth and Environmental Science*, 555: 012050. <https://doi.org/10.1088/1755-1315/555/1/012050>

- [17] Saravanan, R., Maddumala, R. (2020). Alternate heating process in ESP hoppers of thermal power plant-An experimental pilot investigation. In *Advances in Applied Mechanical Engineering: Select Proceedings of ICAMER* 2019, pp. 143-150. https://doi.org/10.1007/978-981-15-1201-8_16
- [18] Kim, S., Chae, T., Lee, Y., Yang, W., Hong, S. (2020). Performance evaluation of a novel thermal power plant process with low-temperature selective catalytic reduction. *Energies*, 13(21): 5558. <https://doi.org/10.3390/en13215558>
- [19] Chichirova, N.D., Abasev, Y.V., Zakirova, I.A. (2020). Digital technologies in the educational process of the thermal power plant department, Kazan state power engineering university. In *2020 V International Conference on Information Technologies in Engineering Education (Inforino)*, Moscow, Russia, pp. 1-4. <https://doi.org/10.1109/Inforino48376.2020.9111756>
- [20] Zhang, J., Zhou, D., Chen, M., Hong, X. (2022). Continual learning for multimode dynamic process monitoring with applications to an ultra-supercritical thermal power plant. *IEEE transactions on Automation Science and Engineering*, 20(1): 137-150. <https://doi.org/10.1109/TASE.2022.3144288>
- [21] Grigor'ev, A.S., Skorlygin, V.V., Grigor'ev, S.A., Mel'nik, D.A., Losev, O.G. (2019). Optimization of a hybrid power plant on the basis of the modeling of thermal processes in it. *Journal of Engineering Physics and Thermophysics*, 92(3): 562-573. <https://doi.org/10.1007/s10891-019-01964-0>
- [22] Weng, F., Zhang, X., Xue, Y., Sun, L. (2022). Deep learning based closed-loop identification of typical thermal process model. In *2022 IEEE 11th Data Driven Control and Learning Systems Conference (DDCLS)*, Chengdu, China, pp. 342-346. <https://doi.org/10.1109/DDCLS55054.2022.9858509>